Analysis of the Microstructure-Properties Relationships of a Quenching & Partitioning Steel: Effect of the Prior Austenite Grain Size

Carola Celada-Casero[1], Piet Kok[2], Wil Spanjer[2], Jilt Sietsma[1] and Maria J. Santofimia[1]
[1]Department of Materials Science and Engineering, Delft University of Technology, Mekelweg 2, 2628CD Delft, The Netherlands
[2]TATA Steel, PO Box 10000, 1970 CA IJmuiden, The Netherlands

Summary: The promising mechanical properties of Quenching & Partitioning (Q&P) steels stem from their complex multi-phase microstructure, which makes it very difficult to unravel the microstructure-properties relationships. This work focuses on the development of 3D models that are able to reproduce average microstructural properties of Q&P steels in order to study their influence on the mechanical response. A cold-rolled 0.2C-3.5Mn-1.5Si (in wt. %) steel was used to design Q&P microstructures with different Prior Austenite Grain Sizes (PAGS). Microstructures were characterized in order to virtually build 3D models using Voronoi tessellations. Crystal plasticity simulations were carried out on the 3D models allowing the identification of possibilities and challenges to develop 3D micro-mechanical models suitable for the complex Q&P microstructures.

Keywords: Q&P, microstructure, mechanical properties, modelling

1. Introduction

The Quenching & Partitioning (Q&P) route involves partial or full austenitisation followed by a quench to a temperature T_Q between the martensite start temperature (M_S) and room temperature (RT) that ensures a controlled formation of martensite. Then, the material is either kept at T_Q or reheated to a higher partitioning temperature (T_P) in order to promote the diffusion of carbon from the martensite to the austenite. With this carbon redistribution, the austenite is stabilized and retained at RT after the final quenching [1]. The refined and highly dislocated martensite contributes to strength and toughness increase, whereas the metastable retained austenite (RA) enhances the work-hardening of the material through the transformation induced plasticity (TRIP) effect.

The Q&P route is regarded as one of the most promising approaches in the development of the third-generation advanced high-strength steels (AHSS) and is just entering the automotive market. It has been demonstrated that the production of certain automotive components via Q&P route could lead to a weight reduction in vehicles and energy saving during the manufacturing [2]. However, the complexity of the Q&P microstructure makes it very difficult to understand the microstructure-properties relationships. Micromechanical simulations of artificial models provide a unique opportunity to study the influence of specific microstructural features on mechanical properties.

The representative volume element (RVE) is a micromechanical modelling concept that helps to understand the influence of microstructure on mechanical properties. It has become very popular, particularly in multi-scale modelling of steel grades,

where the investigations have mainly focused on the study of phase morphologies and spatial distributions [3]. An RVE is a small volume that properly describes the general characteristics of the whole microstructure and in which the states of stress and strain can be approximately considered as homogeneous. An RVE can be defined with a simple Voronoi tessellation that resembles a recrystallized grain structure, but then it will be limited to unrealistic convex shaped grains. The Q&P steels are characterised by complex microstructures, constituted by different phases, morphologies, sizes and distributions [4], and hence the development of realistic microstructural models represents a challenge.

In this study, the influence of the Prior Austenite Grain Size on the mechanical properties of Q&P steels is investigated through micromechanical modelling. The strength of the methodology lies in the strong coupling between microstructure characterization and the creation of representative 3D models. The outcomes and challenges identified in this work represent a step forward to improve the predictive capacity of steel simulations and to make them suitable for Q&P steels.

2. Methodology

2.1. Microstructure design and characterization

A cold-rolled low-carbon steel of composition 0.2C-3.51Mn-1.53Si-0.51Mo (wt.%) was studied in this work. Using a Bähr DIL 805A/D dilatometer, specimens were austenitised at different temperatures (T_γ) to create different PAGSs and, then, subjected to fixed Q&P conditions, as specified in Fig. 1a.

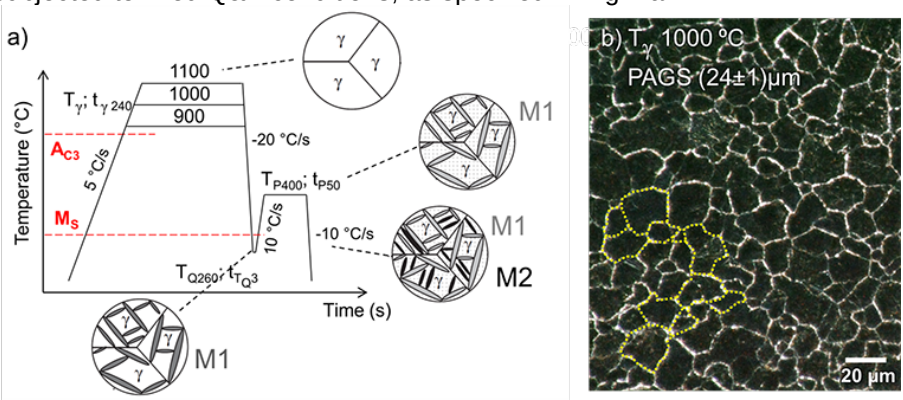

Fig. 1. (a) Q&P route and microstructural evolution. (b) Dark-field LOM micrograph of as-Q specimen austenitised at 1000 °C. M1 stands for martensite formed in the first quench, M2 for martensite formed in the final quench.

The PAGS was revealed by the thermal etching method [5] on specimens quenched to RT from T_γ (as-Q) and determined from dark-field optical micrographs acquired with a Keyence VHX-5000 light optical microscope (LOM) (Fig. 1b). After standard metallographic preparation and etching with 2 % Nital, microstructural inspection of Q&P specimens was done using a JEOL JSM-6500F scanning electron microscope (SEM). The lever rule was applied to the dilatometry data of as-Q specimens to estimate the volume fraction of primary martensite (f_{M1}) formed during the quenching to T_Q = 260°C. Magnetisation measurements were carried out at RT in a vibrating sample magnetometer (LakeShore 7307 VSM) to

determine the volume fraction of retained austenite (f_{RA}) in Q&P specimens, as described in a previous study [6].

2.2. RVE generation

Artificial 3D microstructures are created based on multilevel Voronoi tessellations, which have demonstrated versatility capturing relevant microstructure parameters of multiphase steels [7, 8]. The incorporation of randomness, spatial distributions, grains with complex shapes and different phases is possible. Fig. 2 describes the process to create RVEs. The incorporation of a distribution of realistically shaped grains requires the use of several levels of Voronoi tessellations. First, a fine tessellation of Voronoi cells is created. This is known as the first level and the cells in the first level (n_1) are used as building blocks. Then, a second level is defined by grouping cells of the first level into a coarser tessellation. The coarser tessellation in the second level exhibits more complex and realistically shaped grains (n_2). Finally, a random crystalline orientation distribution is assigned to the grains (second level) in order to reproduce the fully austenitic microstructure. Euler angles are represented with RGB values in the "Texture" frame of Fig. 2. The cells of the first level can also be used to generate particles of other phases with size distributions different from that of the matrix.

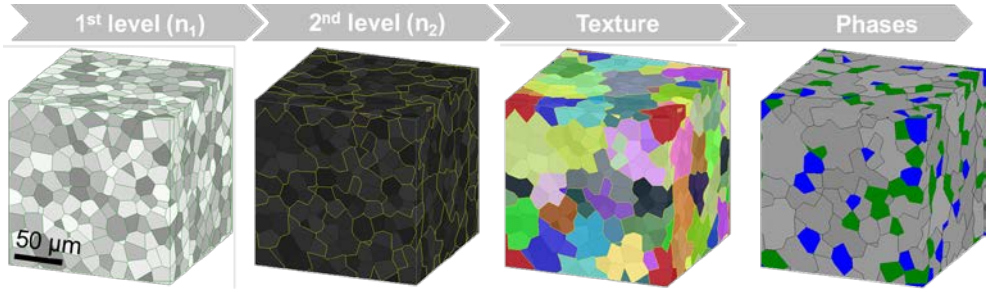

Fig. 2. Summary of steps to build up a microstructure using multilevel Voronoi tessellations

It is easy to recognise the infinite construction possibilities through which the microstructural features can be incorporated in an RVE. Consequently, some question marks arise when designing an RVE. For instance, is there any effect of the RVE size on the mechanical response of the 3D models? Is there any influence of the number of cells in the first level that form a grain in the second level? In parallel to the study of the PAGS effect on the mechanical behaviour, the effect of some parameters determining the Voronoi construction is analysed. In this way, an efficient and suitable way to simulate Q&P microstructures can be identified.

2.3. Crystal plasticity simulations

In order to study the effect of the microstructure on the mechanical properties the cubic models were divided in a regular finite element mesh of 32 x 32 x 32 (= 32768) voxels. The specific phase and crystal orientation for each finite element is assigned in accordance with the location of the cell in the underlying first-level Voronoi tessellation. The created mesh files were simulated using Fourier Spectral Solver software, which makes complex crystal plasticity simulations within a

reasonable time [9]. Outer surfaces of the cubic models are absent by applying periodic boundary conditions.

The integration of RVEs in the micromechanical modelling requires the selection of constitutive model parameters for each phase. The determination of the individual phase and interface properties of Q&P microstructures is one of the remaining challenges to make the models suitable. For this reason, as a first approximation, elastic and plastic parameters of ferrite, martensite and austenite phases were adopted from other studies, in which the deformation behaviour of DP or TRIP steels is investigated [10-12].

For the simulations carried out in this study, all artificial microstructures are subjected to an uniaxial tensile load parallel to the x-direction. A strain rate of 0.006 s^{-1} is applied until a maximum true strain of 14% is reached. The computation of the internal variables is performed incrementally in time in each individual element. After the simulation, the state of stress and strain in each element is obtained. The integration of these points into stress-strain curves gives information of the macroscopic response of the 3D models.

3. Results and discussion

3.1. Characterisation and modelling of Q&P microstructures

Fig. 3 depicts an SEM micrograph of a Q&P microstructure after austenitisation at 1000°C, in which the different microconstituents are highlighted. Table 1 lists the PAGSs and phase volume fractions obtained from the characterisation of the Q&P microstructures. Since no bainite or precipitates form, f_{M2} was estimated by balance. As expected, the PAGS increases with $T\gamma$. It is observed that larger values of f_{M1} are obtained when the PAGS increases, whereas on the contrary the trend for f_{M2} varies. This can be attributed to a mechanical stabilisation of the austenite phase due to a reduction of its grain size [13], which causes a delay in the martensite transformation kinetics. Thus, the quenching of austenite with different grain sizes to the same temperature leads to the formation of different volume fractions of M1. Lower f_{M1} implies lower carbon content available for diffusion into the adjacent austenite during partitioning. Consequently, a lower fraction of austenite is stabilized and larger f_{M2} forms during the final quenching.

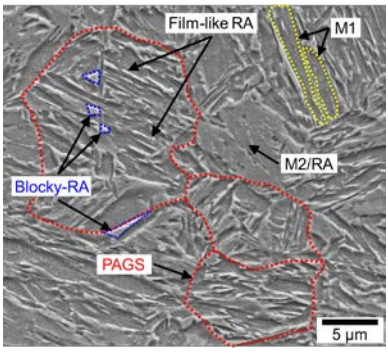

Fig. 3. SEM micrograph of Q&P specimen (T_γ =1000 °C)

Table 1. Microstructural characterisation.
Error of volume fractions is ±0.02

T_γ, °C	900	1000	1100
PAGS, µm	14±1	24±1	67±1
f_{M1}	0.62	0.73	0.81
f_{RA}	0.16	0.15	0.14
f_{M2}	0.22	0.12	0.05

Following the procedure described in *Section 2.2*, 3D RVE models were created incorporating the PAGS and phase volume fractions as characterised in Table 1. The specifications of the models are shown in Table 2 and some examples are displayed in Fig. 4. Since the majority of the austenite transforms into M1 during the first quenching and then is C-depleted during partitioning, the matrix of the final microstructure is not regarded as austenite, but as depleted martensite, represented as ferrite. Therefore, grey grains represent C-depleted martensite / ferrite (M1). In the figure, the orientation distribution of the matrix is not shown so that the RA (green) and M2 (blue) particles can be clearly distinguished.

Table 2. Specifications of various generated RVEs

RVE case	PAGS, μm	RVE side, μm	n_1 (cells)	n_2 (grains)	n_1/n_2	f_{M1} (%)	f_{M2} (%)	f_{RA} (%)
I	14	120	2000	750	3	62	22	16
II	24	118	1000	165	6	73	12	15
III	24	236	4000	1320	3	73	12	15
IV	24	236	7920	1320	6	73	12	15
V	67	215	1000	50	20	79	7	14

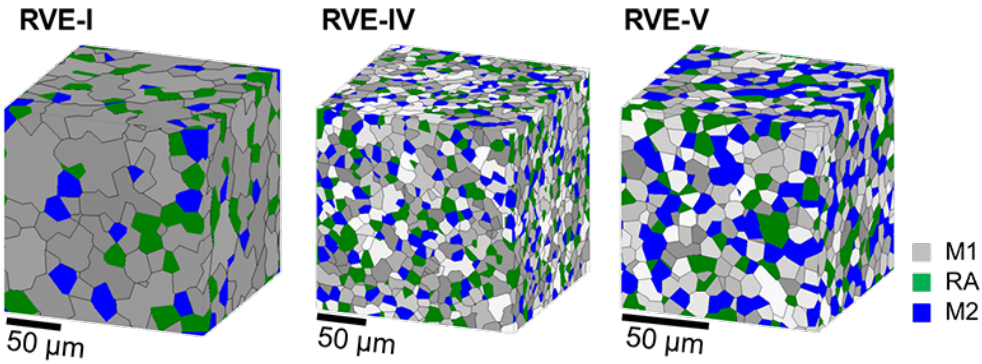

Fig. 4. Periodic 3D RVEs of cases I, IV and V (Table 2). For colour interpretation, the reader is referred to the online version.

In order to study the influence of the Voronoi construction parameters on the flow behaviour, additional RVEs were created to isolate some effects (Table 2). For instance, by comparing cases II and IV, it is possible to study the effect of the RVE size on the flow behaviour. On the other hand, the comparison between RVE-III and RVE-IV allows for the investigation of the influence of the ratio n_1/n_2; that is the influence of the number of cells in the first level (n_1) constituting grains in the second level (n_2).

3.2. Simulation of the mechanical response to uniaxial loading

The mechanical response to uniaxial load until 14% deformation was simulated in all RVEs. As example, Fig. 5 depicts the results obtained for model RVE-I. The centre and right-hand models show the strain and Cauchy stress distributions, respectively. The results are not smooth due to the coarse selected mesh size but the accuracy is sufficient to study the average response of the structure. The

elongation experience by the models due to plastic deformation is appreciated in the x-direction. The strain and stress distributions are complementary. Whereas higher strain is experienced by the M1 matrix, the concentration of stress is more pronounced in the particles of M2. This is reasonable since the M2 lattice is more distorted due to a higher carbon concentration and dislocations density than M1, which makes M2 harder and higher stress is required for its plastic deformation. On the contrary, the carbon content in M1 is very low and its flow stress is mainly controlled by the orientation distributions and grain size.

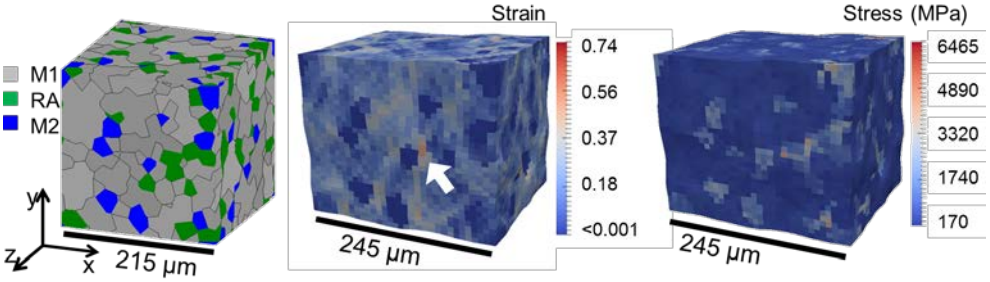

Fig. 5. RVE-I (PAGS = 67 µm) before (left) and after (centre and right) 14% uniaxial deformation, where the effect of the phases and orientations on strain and Cauchy stress distribution is observed.

The effect of grain boundaries as obstacles to dislocation motion is not captured by crystal plasticity simulations within a finite-strain continuum mechanical framework. The effect of the grain size is captured by the different orientations of the grains. Grains of different orientations have different stiffness, which leads to strain gradients between grains. The distribution of the M2 phase plays a role in the development of strain gradients in M1. As pointed by the white arrow, high strain in M1 appears located in between particles of different nature that are very close to each other. The role of the RA is not clear. Instead of providing ductility, its behaves as a secondary phase. This indicates that the understanding of the constitutive behaviour of RA requires further investigation.

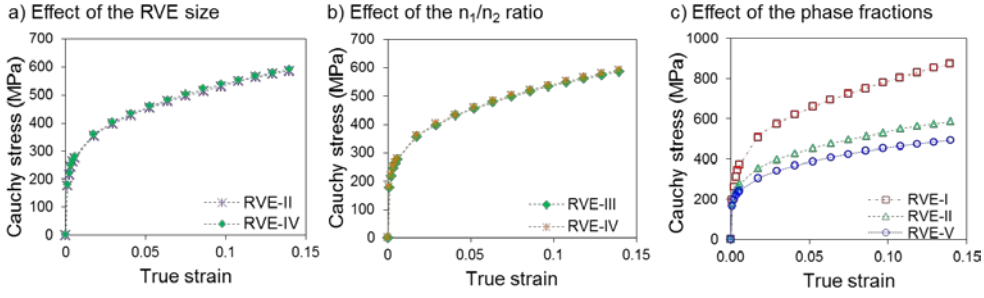

Fig. 6. Flow curves of the RVE models specified in Table 2: a) Effect of the RVE cube size, b) effect of the number of cells constituting each grain and c) effect of the PAGS and volume fraction of phases.

The mechanical response of all RVE models was integrated into stress-strain curves, shown in Fig. 6. Fig. 6a and b point out that there is no effect on the mechanical behaviour of the RVE size, nor of the number of cells per grain (ratio n_1/n_2) used in the tessellations. This first conclusion has an important implication: the size of the RVEs can be reduced and still capture the representative microstructural parameters. By reducing the size of the RVE, the resolution of the

simulations can be enhanced and the computational time decreased. The conclusion drawn from Fig. 6b requires careful interpretation. If the number of cells constituting the grains is reduced below a certain number, the grains lose their realistic morphology and this may be reflected in the mechanical behaviour. Finally, Fig. 6c shows the effect of phase volume fractions as a consequence of a different microstructural evolution during the Q&P route originating from differences in the PAGS. As expected, the larger f_{M2} (hard phase), the higher the strength.

3.3. Challenges

In this work, the microstructural modelling of Q&P structures is investigated with the aim of developing a micromechanical model that allows for the understanding of microstructure-properties relationships in Q&P steels. The predictive capacity of the simulations has improved significantly in recent years, especially for DP steels. However, the quality of the models is not sufficient yet for Q&P microstructures and, therefore, the flow curves predicted in this work are not realistic or representative. This investigation identifies some important challenges to address if models suitable for Q&P steels are sought:

1) *Determination of the flow properties of individual Q&P microconstituents*. To this end, it is crucial to understand the metallurgical processes behind the Q&P route. In this sense, the redistribution of carbon during the partitioning is of special importance. The strengthening of the C-depleted and secondary martensite phases [14] as well as the stability of the austenite phase [15, 16] directly depend on their carbon content. To determine the constitutive properties of Q&P microconstituents, theoretical models need to be developed and further experimental characterisation is required, for instance by nanoindentation.

2) *Crystallography and morphology of phases*. The RVE models represent the C-depleted ferritic matrix (M1) as grains of different orientations, which does not represent the hierarchical martensitic structure constituted by packets, blocks and laths. During mechanical simulations, the strain gradients in the RVE's matrix are built based on their grain orientations, which are homogeneous across the whole grain. This is not the case for real martensitic microstructures, in which packets, blocks and laths have specific orientation relationships among them and with the parent austenite [17]. Different strain gradients may be generated during the simulations if the crystallography and morphology of martensite and RA are considered in the 3D models.

.

4. Conclusions

The effect of the PAGS on the mechanical behaviour was studied in a Q&P steel. Differences in the PAGS result in different phase volume fractions during the Q&P route. RVEs were modelled capturing the phase volume fractions of the real Q&P microstructures and their response to uniaxial loading was simulated. An increase in the strength is observed as the volume fraction of secondary martensite increases in the microstructure. However, the flow behaviour obtained from the models is not realistic due to mainly two reasons: (1) the constitutive behaviour of the individual Q&P microsconstituents is not sufficiently understood yet, and (2)

models do not properly capture the hierarchical structure of the Q&P microconstituents.

Additionally, it was observed that the efficiency of RVE modelling can be improved by reducing their size, which will increase the local accuracy of stress and strain distribution and reduce the computational time.

5. Acknowledgments

The authors deeply acknowledge the support from the Research Fund for Coal for funding this research under the Contract RFCS-02-2015 (Project No. 709755).

References

[1] Speer, J. G., Assunção, F. C. R., Matlock, D. K. and Edmonds, D. V.: Mater. Res., 417-423 (2005), 8.
[2] New high-strength, room-temperature-formable steels sought. SAE Int.: 06-Aug.e.(2013).
[3] Amirmaleki, M., Samei, J., Green, D. E., van Riemsdijk, I. and Stewart, L.: Mec. Mater., 27-39 (2016), 101.
[4] Santofimia, M. J., Zhao, L., Petrov, R., Kwakernaak, C., Sloof, W. G. and Sietsma, J.: Acta Mater., 6059-6068 (2011), 59.
[5] San Martín, D., Palizdar, Y., Cochrane, R. C., Brydson, R. and Scott, A. J.: Mater. Charact., 584-588 (2010), 61.
[6] Zhao, L., van Dijk, N. H., Brück, E., Sietsma, J. and van der Zwaag, S.: Mater. Sci. Eng. A, 145-152 (2001), 313.
[7] Yadegari, S., Turteltaub, S., Suiker, A. S. J. and Kok, P. J. J.: Comp. Mater. Sci., 339-349 (2014), 84.
[8] Kok, P. J. J., Spanjer, W. and Vegter, H.: KEM, 975-980 (2015), 651-653.
[9] Roters, F., Eisenlohr, P., Kords, C., Tjahjanto, D. D., Diehl, M. and Raabe, D.: Procedia IUTAM, 3-10 (2012), 3.
[10] Maresca, F., Kouznetsova, V. G. and Geers, M. G. D.: J. Mech. Phys. Solids, 69-83 (2014), 73.
[11] Tasan, C. C., Hoefnagels, J. P. M., Diehl, M., Yan, D., Roters, F. and Raabe, D.: Int. J. Plasticity, 198-210 (2014), 63.
[12] Maresca, F., Kouznetsova, V. G. and Geers, M. G. D.: Mec. Mater., 198-210 (2016), 92.
[13] Chatterjee, S., Wang, H. S., Yang, J. R. and Bhadeshia, H. K. D. H.: Mater. Sci. Tech., 641-644 (2006), 22.
[14] Rodriguez, R.-M. and Gutierrez, I.: Mater. Sci. Forum, 4525-4530 (2003), 426-432.
[15] Jacques, P. J., Delannay, F. and Ladrière, J.: Metall. Mater. Trans. A, 2759-2768 (2001), 32.
[16] Wang, J. and Van Der Zwaag, S.: Metall. Mater. Trans. A, 1527-1539 (2001), 32.
[17] Morito, S., Tanaka, H., Konishi, R., Furuhara, T. and Maki, T.: Acta Mater., 1789-1799 (2003), 51.